Journal of Engineering and Applied Sciences 14 (22): 8282-8288, 2019
ISSN: 1816-949X

Detection and Localization of Multiple Targets in a MIMO System using DFT Wideband Waveforms

[1]Raed S.M. Daraghma and [2]Nuray At
[1]Department of Electrical and Electronics Engineering, Palestine Technical University
Palestine, Tulkarm
[2]Department of Electrical and Electronics Engineering, Anadolu University, Eskisehir, Turkey
R.daraghmeh@ptuk.edu.ps

Abstract: In this study, we address the problem of Direction of Departure (DOD) and Direction of Arrival (DOA) estimation for moving targets and waveform design techniques of bistatic Multiple Input Multiple Output (MIMO) radar. The research presented studies an efficient estimation of the target DOA and DOD with automatic pairing. In this research, we aim at reducing the average angular error. To make better decisions in error performance, we design and implement a new technique by using discrete Fourier transform. This technique can effectively reduce error in the detection and localization of the multiple targets in a MIMO system. The simulation results of the proposed algorithm are presented and the performances are investigated and discussed. It is seen that the steering vectors of moving targets for bistatic MIMO radar using Discrete Fourier Transform (DFT) can pair the estimated angles easily. Furthermore, we enhance the DOA estimation performance in the wideband state. As a result, our procedure achieves better estimation performance than Capon, Multiple Signal Classification (MUSIC) and Parallel Factor analysis (PARAFAC) and it has better angle estimation.

Key words: MIMO radar, DFT, Parallel Factor (PARAFC), Direction of Arrival, DOD, wideband state

INTRODUCTION

Multiple-Input Multiple-Output (MIMO) radar uses multiple transmitter and various receiver elements. In the last years, MIMO radar systems have be used for many applications including both fields military and civilian (Lesturgie, 2011; Martinez-Vazquez and Fortuny-Guasch, 2007). Capon (1969) selected a number of different moving targets: simple and complex targets with different RCS and speeds. From the presenting work on the implementation of Capon, MUSIC and PARAFAC to the localization of different targets, he noticed the importance of the types of targets and the effect of changing the speed of targets.

The MUISC technique, Schmidt (1986) and Parallel Factor (PARAFAC) technique. Even though narrow band MIMO radar has been deeply inspected in the latest years, the hypothesis done in the signal paradigm larger run in the state of wide band signals. One of the major advantage in the MIMO radar system is a waveform design. The efficiency of transmitting distinct waveforms for all elements of the array improve the angular and range resolution and the target parameter identification. Additionally, improvement in resolution and maximization in Signal to Noise Ratio (SNR) can be gained by the employ of wideband signals on transmission beam patterns. PARAFAC shows robust distinction properties without forcing orthogonality of the loading vectors. PARAFAC is one likely popularization of the matrix unique value decomposition to higher arrangement state. PARAFAC analysis and signal processing materials depend on multi-linear tensor algebra give us to employ the robust algebra framework of these multidimensional signals (Schmidt, 1986; Kruskal, 1977; Sidiropoulos and Bro, 2000). By Stegeman and Sidiropoulos (2007) the PARAFAC analysis, the researcher shows that the detection and localization of various targets can alternatively be accomplished, PARAFAC mechanism is defined and utilizes the algebraic framework of the received data where Radar Cross Section (RCS) variation are not considered as an annoyance variable but kind of origin of time variety. In this study, we choose PARAFAC to decomposition the three-way tensor of the received to get the directional matrices of arrival and departure. From the present research on the implementation of PARAFAC to the localization of targets, we can notice that it fundamentally submitted for far-filed narrowband target location. In this study, we expand it to far-filed wideband state.

Corresponding Author: Raed S.M. Daraghma, Department of Electrical and Electronics Engineering, Palestine Technical University, Palestine, Tulkarm, R.daraghmeh@ptuk.edu.ps

Nion and Sidiropoulos (2009) addressed the DOA estimation problem with non-orthogonal signals in MIMO radar system. Researcher analyses the effect of number of targets for MUSIC technique. Also, CRLB for non-orthogonal signals has been given. Licul and Davis (2005) addressed the problem of target detection in phased MIMO radar, the closed form expression of the false alarm and detection probabilities in the existence of Gaussian noise are given.

Problem statment: MIMO narrow band signals have been studied in the literatures for several targets, the implementation of DOA estimation of moving targets and waveform purposes for MIMO radar have been studied. In this research, our objective is to survey the present DOA estimation and waveform layout mechanisms and to improve novel technique to develop new signal algorithm to improve the DOA estimation performance for moving targets depending on wideband signals. In this research, the narrowband signal pattern for plane wave areas of far-field are qualified, next our wideband signal pattern is presented and it is performance is analyzed with different well known algorithm such as PARAFAC.

MATERIALS AND METHODS

MIMO radar signal model: In this study, we have considered Coherent Processing Interval (CPI) be formed of Q consecutive pulse periods and Swelling II target pattern was assumed where it is deferring from pulse to pulse. The targets are located in the far-field. The baseband received signal at the output of the receive configuration after synchronization can be noted as:

$$X_q = B(\varnothing)\Sigma_q A^T(\theta)S+W_q \quad (1)$$

q = 1, 2, …, Q where, $X_q \in R^{M_t \times L}$, combines the L samples received by M_r antennas for the qth pulse interval $\sum_q$ diag (C_q) with $c_q = [\delta_{1q}, \ldots, \delta_{kq}]$, $\delta_{kq} = \alpha_{kq}\, e^{j(q-1)x}$, i.e., x_q is the Doppler frequency of the kth target. The RCS coefficients δ_{kq}, k = 1, …, K are altering independently from pulse to pulse and $W_q \in R^{M_t \times L}$ is the noise interference term. MIMO radar transmits mutually orthogonal waveforms. We suppose that $1/SLS^H = I_M$. Next proper multiplication of (Eq. 1) by $(1/L)S^*S^H$, the matched filter output is:

$$Y_q = B(\varnothing)\Sigma_q A^T(\theta) + Z_q \quad (2)$$

$$Y_q = \frac{1}{LXS^H} \in C^{M_r \times M_t},\ Z_q = \frac{1}{LWS^H}$$

Let us factorize (Eq. 2):

$$Y_q = \left(A(\varphi)\square\ B(\theta)C_q^T + Z_q\right) \quad (3)$$

$Y_q = vec(Y_q)$, $Z_q = vec(Z_q)$ which can be formed in the close shape:

$$Y = (A(\varphi)\square\ B(\theta)C^T + Z \quad (4)$$

$Y = [Y_q, \ldots, Y_Q]$ and $Z = [Z_q, \ldots, Z_Q]$ are of size $M_tM_r \times Q$ and $C^T = [C_1^T, \ldots, C_Q^T]$ is of size $K \times Q$.

Data model: The waveform design is one of the major issue of concern in the subject of MIMO radar, actually wideband signal waveforms improve the estimation of multi-target variables such as range, doppler, Direction of Arrival (DOA) and reflection coefficients. In the narrowband state, the transmit steering vector relies only on the direction ⌀ of the wave front and can be given by:

$$a_t(\varnothing) = \frac{1}{R}e^{\frac{2\pi}{\lambda}(D\sin\varnothing + H\cos\varnothing)}[g^*_{t,i}(\varnothing)e^{\frac{2\pi}{\lambda}\left(\frac{M_t-1}{2}-i\right)\frac{d_t\sin\varnothing}{v}}]_{i=0,\ldots,M_t-1} \quad (5)$$

Let us consider MIMO radar where, M_t, M_r transmitting and receiving antennas are collocated. Assume the target suited at (⌀, R), the received baseband signal at the M antenna segment of the receive discipline, extracted from the electric field mode is noted by:

$$x_m(t) = \frac{\mu_{0\beta e j k_m^T r_m}}{4\pi\|r_m\|}[h_{r,m}((U_{rm,t}) * \sum_{1=0}^{M_{t-1}} \frac{h_{t,i}(U_{rm,t})}{\|r_i\|} * C_i(t-\tau_i-\tau_m)e^{j(2\pi f_C t - K_i^T r_i)})]e^{-j2\pi f_C t} + Z_m(t) \quad (6)$$

m = 0, ..., M_t-1 where, $\tau_i = K_i^T r_m / 2\pi f_C$, $\tau_m = K_m^T r_m / 2\pi f_C$ and Z(t) is the noise and interfrence recived by mth antenna element. Equation 6 can be rewritten by :

$$x_m(t) = \frac{\mu_{0\beta e - jk_m^T r_m}\left(1+\frac{f}{f_C}\right)\mu_0\beta e^{-jk_m^T r_m}\left(1+\frac{f}{f_C}\right)}{4\pi\|r_m\|} [H_{r,m}][(U_{rm,f+f_C}) * \sum_{1=0}^{M_{t-1}} \frac{H_{t,i}(U_{rm,f+f_C})}{\|r_i\|} e^{-jk_i^T r} \left(1+\frac{f}{f_C}\right) C_i(f)] + Z_m(f) \quad (7)$$

The antenna radiation pattern (Eq. 7) is given by:

$$x_m(f)=\alpha\beta\frac{1}{\|r_m\|}e^{-jk_m^T r_m\left(1+\frac{f}{f_C}\right)}g_{r,\,m}(\varnothing,\,f+f_C)\sum_{i=0}^{M_t-1}\frac{1}{\|r_i\|}g_{r,\,m}(\varnothing,\,f+f_C)e^{-jk_i^T r\left(1+\frac{f}{f_C}\right)}C_i(f) \quad (8)$$

$$X(f)=\left[X_0(f),\,...,\,X_{M_r-1}(f)\right]^T,\quad C(f)=\left[C_0(f),\,...,\,C_{M_r-1}(f)\right]^T,\quad Z(f)=\left[Z_0(f),\,...,\,Z_{M_r-1}(f)\right]^T$$

$$a_t(\varnothing,f)=\frac{1}{R}e^{j2\pi\left(\frac{f+f_C}{v}\right)(D\sin\varnothing+H\cos\varnothing)}\left[g_{t,\,i}^*(\varnothing,f,f_C)e^{j2\pi(f,\,f_C)\left(\frac{M_{t-1}}{2}-i\right)\frac{d_t\sin\varnothing}{v}}\right]_{i=0,\,...,\,M_t-1} \quad (9)$$

$$a_r(\varnothing,f)=\frac{1}{R}e^{j2\pi\left(\frac{f+f_C}{v}\right)(D\sin\varnothing+H\cos\varnothing)}\left[g_{r,\,i}^*(\varnothing,f,f_C)e^{j2\pi(f,\,f_C)\left(\frac{M_{r-1}}{2}-i\right)\frac{d_r\sin\varnothing}{v}}\right]_{i=0,\,...,\,M_r-1} \quad (10)$$

The DOA estimation mechanisms will be carry out by two dimension consider parameters ($\varnothing$, f) in the plane wave state the product $K_i^T r_i$ is given by:

$$K_i^T r_i=\frac{2\pi f_C}{v}\left(D-\left(i-\frac{M_t-1}{2}\right)dt\right)\sin\varnothing+\frac{2\pi f_C}{v}H\cos\varnothing\;i=0,\,....,\,M_t-1 \quad (11)$$

The wideband signal pattern in the state of K targets existed in the plane wave area is given in frequency domain as:

$$X(f)=\sum_{k=1}^{K}\beta_k a_r^*(\varnothing_k,f)a_t^H(\varnothing_k,f)C(f)+Z(f) \quad (12)$$

The DOA estimation should be executed over the entire frequency band employing discrete frequencies, thus, it is convenient to count the Discrete Fourier Transform (DFT) of $\{x_m(n)\}_{n=0}^{N-1}$:

$$x_m(p)=\sum_{n=0}^{N-1}x_m(n)\,e^{-j2\pi\frac{n}{p}\left(p-\frac{n}{2}\right)p}\quad P=0,\,....,\,N-1 \quad (13)$$

Consequently, Eq. 13 can be formed as in discrete frequency domain as:

$$X(p)\cong\sum_{k=1}^{K}\beta_k a_r^*(\varnothing_k,f)a_t^H(\varnothing_k,f)C(f)+Z(f)\quad p=0,\,...,\,N-1 \quad (14)$$

$$a_t(\varnothing_k,f)=\left[g_{t,\,i}^*(\varnothing,f+f_C)e^{j2\pi\left(f_c+f_p\right)\left(\frac{M_t-1}{2}-i\right)\frac{d_t\sin\varnothing}{v}}\right]_{i=0,\,...,\,M_t-1} \quad (15)$$

$$a_r(\varnothing_k,f)=\left[g_{r,\,i}^*(\varnothing,f_p+f_C)e^{j2\pi\left(f_c+f_p\right)\left(\frac{M_r-1}{2}-i\right)\frac{d_r\sin\varnothing}{v}}\right]_{i=0,\,...,\,M_r-1} \quad (16)$$

where:

$$f_p=\frac{PF_S}{N}-\frac{F_S}{2},\quad X(P)=\left[X_0(p),\,...,\,X_{M_r-1}(p)\right]^T,\quad C(P)=\left[C(p),\,...,\,C_{M_r}-1(p)\right]^T,\quad Z(P)=\left[C(p),\,....,Z_{M_r}-1(p)\right]$$

are the DFT (element-wise) of x(n), c(n) and z(n), respectively.

RESULTS AND DISCUSSION

In this study, MATLAB program simulation results are presented to verify the above analysis and compare the performance of our technique with PARAFAC technique. Localization of the numerous targets for a uniform linear configuration layout at the transmitter and receiver can be attained by the above techniques (Nion and Sidiropoulos, 2009). We generate the matrices S, A and B as demonstrated in the previous section. S is produced by $(S)_m$ = (1+j/2)$[H]_m$ where, ... is the N×N Hadamard matrix and N is bounded to 256. The Signal to Noise Ratio (SNR) at the receiver is outlined as:

$$SNR=10\log\left(\sum_{q=1}^{Q}\left\|B\sum_q A^T S\right\|^2 F/\|W\|^2 F\right)dB$$

where, Additive White Gaussian Noise (AWGN) is supposed and $\|.\|_F$ is the Frobenis norm. We choose ULA transmit and receive configurations with $\lambda/2$ interelement interval for both configurations. For the Swerling II target pattern, each column of the matrix $C\epsilon Ç^{Q\times K}$ is created from a sophisticated Gaussian distribution with zero mean and variance $\sigma^2_{\delta k}$ where, δ_K is sample drawn from a complex Gaussian distribution with zero mean and variance $\sigma^2_{\delta k}$ and the Doppler frequency X_K is produced by:

$$X_k=\frac{2\pi V_k T_p}{\lambda}$$

Where:

V_K = The target speed

T_p = The 5×10^{-6} is the pulse duration (sec)

λ = The $3\times10^8/f_c$ (GHz)

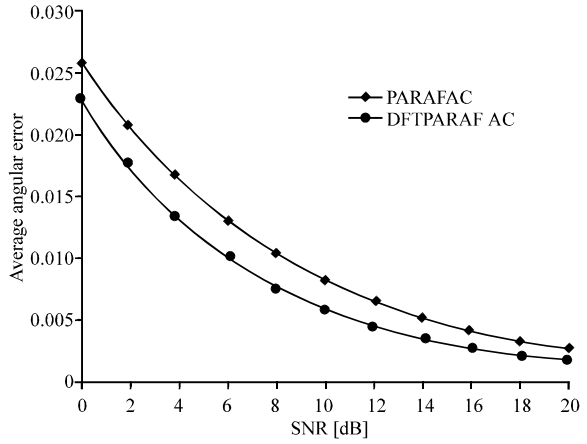

Fig. 1: Swerling II multiple-pulses bistatic MIMO layout, differentiation between PARAFC and DFT-PARAFC. Q = 200 pulses, L = 512 samples. k = 2 targets velocities {300 and 250 msec^{-1}}

This subsection analyzes the influence of the number of targets on the performance detection. The rendering. standard is the absolute value of the difference between the true angle and estimated angle, averaged over transmit and receive angles and over all targets. In a first experiment (Fig. 1), we compare the performance of PARFAC based procedure to the our DFT-PARAFC. In Fig. 1, we have plotted the PARAFAC pattern and DFT-PARAFC, for k = 2 targets with DODs [-10^0, -14^0] and DOAs [20^0, -24^0], the set $\{\sigma^2_\delta K\}^K_{k=1}$ = {0.35,0.4}, Q = 200 pulses, L = 512 samples and swerling II pattern is selected with M_t = 8 transmit and M_r = 8 receive antennas, performance is assessed in the cases SNR from {0-20 dB}, for each value of the SNR, we compare both procedures via. 100 Monte Carlo simulation as expected the performance of the two procedures the average angular error increases when the value of SNR increases, we observe the DFT- PARAFC outperforms PARAFC at all values of SNR.

In Fig. 2, we have plotted the PARAFAC pattern and DFT-PARAFC, for k = 6 widely spaced targets with DODs [-80^0, -60^0, -40^0, -20^0.0^0, 20^0] and DOA [70^0, 10^0, 50^0, -30^0, -10^0, 30^0], the set $\{\sigma^2_\delta K\}^K_{k=1}$ = {0.35, 0.4, 0.45, 0.55, 0.6}, Q = 50 pulses, L = 512 samples and swerling II pattern is selected with M_t = 8 transmit and M_r = 8 receive antennas, performance is assessed in the cases SNR from {0-10 dB}, for each value of the SNR, we compare both procedures via. 100 Monte Carlo simulation as expected the performance of the two procedures the average angular error increases when the value of SNR increases, we observe the DFT-PARAFC outperforms PARAFC at all values of SNR.

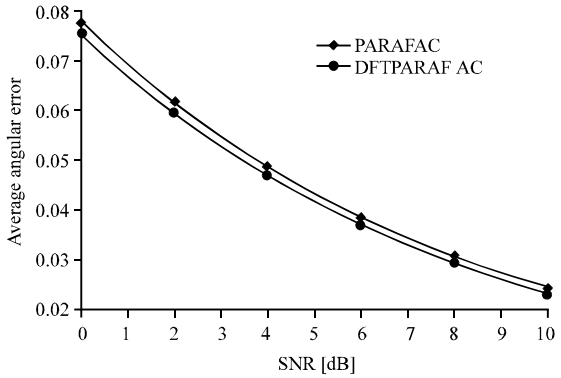

Fig. 2: Swerling II multiple-pulses bistatic MIMO layout, differentiation between PARAFC and DFT-PARAFC. Q = 200 pulses, L = 512 samples. k = 6 targets. Widely spaced case velocities {300, 250, 200, 250, 350 and 300 msec^{-1}}

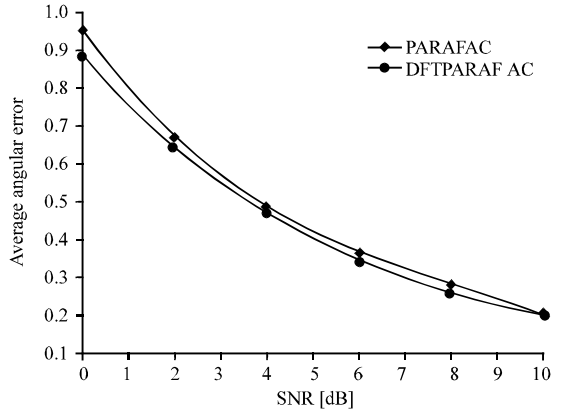

Fig. 3: Swerling II multiple-pulses bistatic MIMO layout, differentiation between PARAFC and DFT-PARAFC. Q = 50 pulses, L = 512 samples. k = 6 targets, closely spaced case, velocities {300, 250, 200, 250, 350 and 300 msec^{-1}}

In Fig. 3, we have plotted the PARAFAC pattern and DFT-PARAFC, for k = 6 closely spaced targets with DODs [-80^0, -75^0, -40^0, -35^0, 0^0, 5^0] and DOAs [70^0, 65^0, 50^0, 45^0, -10^0, -15^0], the set $\{\sigma^2_\delta K\}^K_{k=1}$ = {0.35, 0.4, 0.45, 0.5, 0.55, 0.6}, Q = 50 pulses, L = 512 samples and swerling II pattern is selected with M_t = 8 transmit and M_r = 8 receive antennas, performance is assessed in the cases SNR from {0-10 dB}, for each value of the SNR, we compare both procedures via. 100 Monte Carlo simulation as expected the performance of the two procedures the average angular error increases when the value of SNR increases. We observe the DFT-PARAFC outperforms PARAFC at all values of SNR.

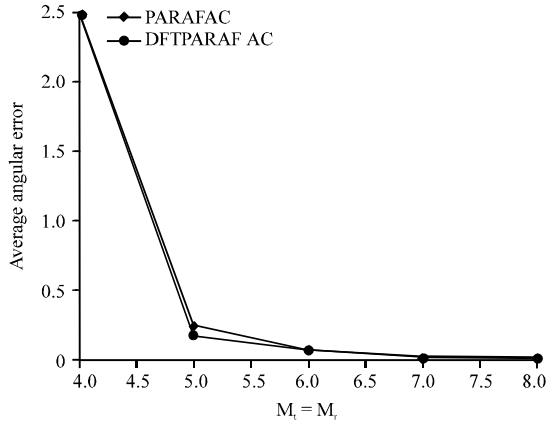

Fig. 4: Effect of the number of antennas on the performance of PARAFAC and DFT-PARAFAC

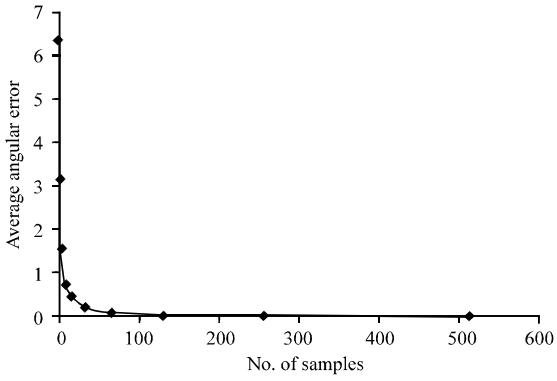

Fig. 5: Effect of the number of samples for each transmitted pulse on the performance of DFT-PARAFAC

In Fig. 4, we have plotted the DFT-PARAFC, for k = 2 targets with DODs [-10^0, -14^0] and DOAs [-20^0, -24^0], the set $\{\sigma^2_\delta K\}^K_{k=1}$ = {0.35,0.4}, Q = 200 pulses and swerling II pattern is selected with $M_t = M_r = 2$ transmit and receive antennas, performance is assessed in the cases SNR is set to 10 dB, for each value of the transmit and receive antenna, the average angular error decrease when the number of samples for each transmitted pulse increases.

In Fig. 5, we plot the true angles for the three targets (k = 3), the target type is fighter with DODs [-80^0, -40^0, 0^0] and DOAs [70^0, 50^0, -10^0], the set $\{\sigma^2_\delta K\}^K_{k=1}$ = {40, 40, 40}, speed {125, 125, 125}, Q = 100 pulses, the number of samples for each transmitted pulse is changed and swerling II pattern is selected with $M_t = M_r = 3$ transmit and receive antennas, performance is assessed in the cases SNR is set to 10 dB. For Fig. 6, true angles for the three targets are plotted. In Fig. 7 and 8, we differentiate the rendering of several localization mechanisms via. Monte Carlo simulations.

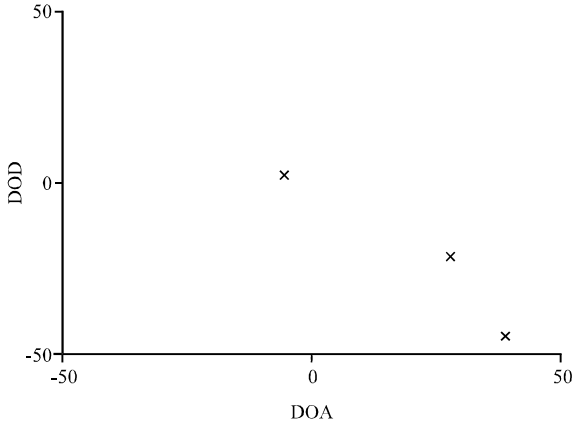

Fig. 6: True angles for the three targets

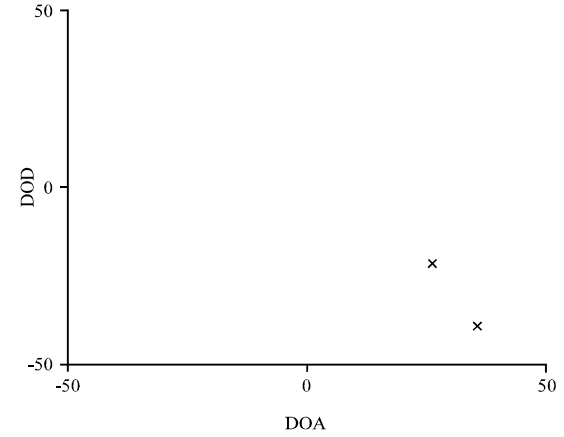

Fig. 7: Localization of the three targets by using two-way Capon technique (SNR = 10 dB)

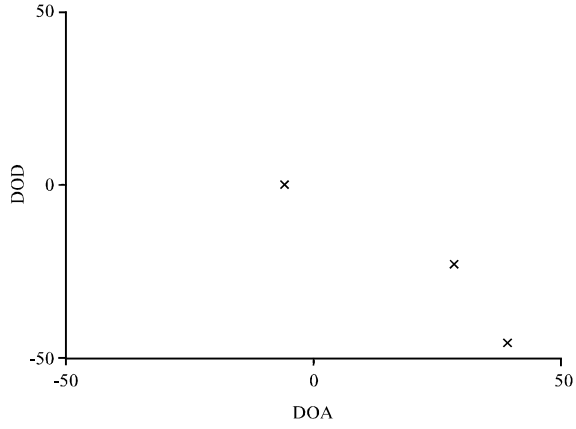

Fig. 8: Localization of the three targets by using DFT two-way Capon technique (SNR = 10 dB)

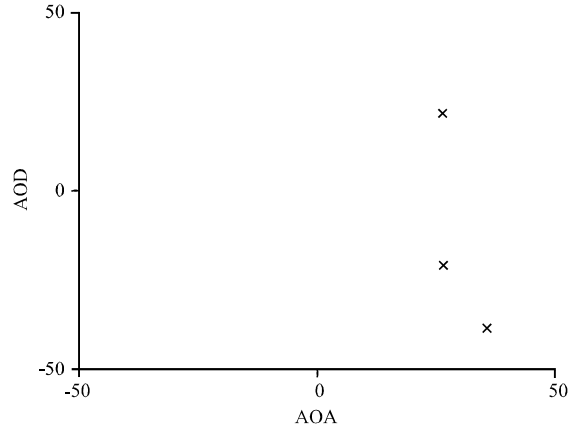

Fig. 9: Localization of the four targets by using two-way Music technique (SNR = 10 dB)

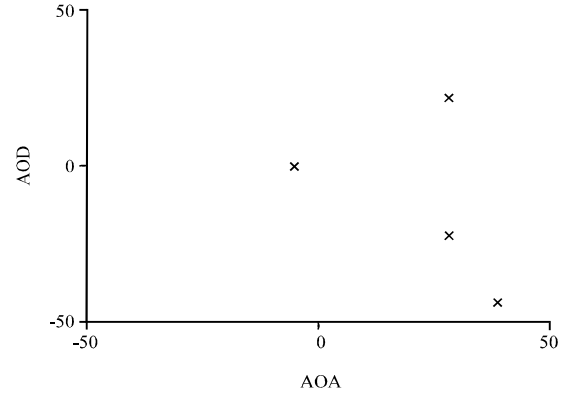

Fig. 10: Localization of the four targets by using DFT two-way Music technique (SNR = 10 dB)

In Fig. 7 and 8, we have plotted the two-way capon, DFT two-way capon. For the simile between two procedures to be adjuster, the angular resolution of the two subsequent mechanisms is bounded to 0.001^0. In Fig. 7, we can see form three targets, two-way capon technique can detect two targets from the three targets (one target is missing). From Fig. 8, we can see the DFT two-way capon technique can detect the three targets. From these results, we can conclude that the superiority of using DFT with the two-way capon technique.

In Fig. 9 and 10, we compare the performance of several localization mechanisms via. Monte Carlo simulations. In Fig. 9, we can see form four targets, two-way Music technique can detect three targets from the four targets (one target is missing). From Fig. 10, we can see the DFT two-way Music technique can detect the four targets. From these results, we can conclude that the superiority of using DFT with the two-way Music technique.

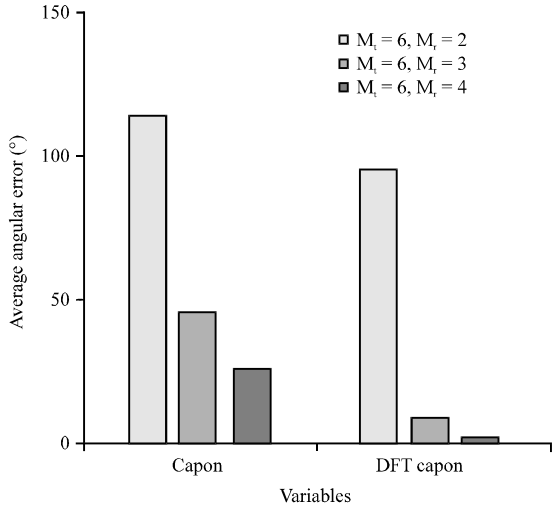

Fig. 11: Multiple-pulses bistatic MIMO configuration, comparison between Capon and DFT-Capon

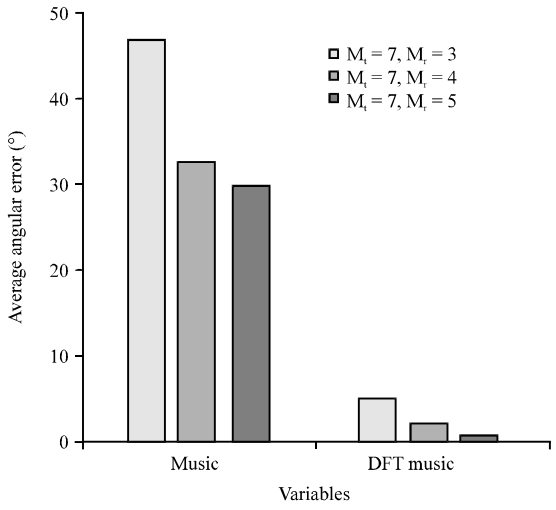

Fig. 12: Multiple-pulses bistatic MIMO configuration, comparison between Music and DFT-Music

In Fig. 11, we compare the performance of Capon based procedure to the our DFT-Capon, we have plotted the Capon pattern and DFT-Capon, for k = 6 targets with DODs [-80^0, -40^0, 0^0, 20^0, -40^0, -60^0] and DOAs [70^0, 50^0, -10^0, 30^0, -25^0, 20^0], the set $\{\sigma^2_8 K\}^K_{k=1}$ = [40, 40, 40, 40, 40, 40], Q = 100 pulses, L = 512 samples, SNR = 10 dB, speed = [125, 125, 125, 125, 125, 125] and swerling II pattern is selected with M_t = 6 transmit and M_r = 2-4 receive, we compare both procedures via. 100 Monte Carlo simulation as expected the performance of the two procedures the average angular error decreases when the value of M_t and M_t increases, we observe the DFT-Capon outperforms Capon at all values of M_t and M_t (Fig. 12).

In Fig. 12, we compare the performance of Music based procedure to the our DFT-Music, we have plotted the Music pattern and DFT-Music, for k = 7 targets with DODs [-80^0, -40^0, 0^0, 20^0, -40^0, -60^0, 30^0] and DOAs [0^0, 50^0, -10^0, 30^0, -25^0, 20^0, 40^0], the set $\{\sigma^2_s K\}^K_{k=1}$ = [40, 40, 40, 40, 40, 40, 40], Q = 100 pulses, L = 512 samples, SNR = 10 dB, speed = [125, 125, 125, 125, 125, 125, 125] and swerling II pattern is selected with M_t = 7 transmit and M_r = 3-5 receive, we compare both procedures via. 100 Monte Carlo simulation as expected the performance of the two procedures the average angular error decreases when the value of M_t and M_r increases, we observe the DFT-Music outperforms Music at all values of M_t and M_r.

CONCLUSION

In this study, we have considered the detection and localization of moving target in bistatic MIMO radar with both cases: closely and widely separated antennas where multiple antennas transmit linearly independent waveforms and multiple antenna receive the reflected signal. MIMO radar system can be an accomplished by the PARAFAC decomposition of the observed data tensor. In general, previous researches showed that the resolution and performance of parallel factor is affected by cross talk or interference which correlated with the transmitted signals. In order to overcome this problem, we used narrowband MIMO radar with DFT algorithm. The DOA estimation performance is greatly improved. Moreover, we showed that using DFT allows improving the DOA estimation performance of Capon, Music and the parallel factor, simulation results illustrate the potential of our technique which outperforms the normal Capon, Music and PARAFAC procedures.

AKNOWLEDEGEMENT

We would say to thank for those support our research. The organization that support our research is WELFARE (Taawon) and Bank of Palestine foundations. We sincerely thank the Anonymous reviewers for their constructive comments and suggestions. I never forget, my deep thank for my university: Palestine Technical University Kadoorei.

REFERENCES

Capon, J., 1969. High-resolution frequency-wave number spectrum analysis. Proc. IEEE, 57: 1408-1418.

Kruskal, J.B., 1977. Three-way arrays: Rank and uniqueness of trilinear decompositions, with application to arithmetic complexity and statistics. Linear Algebra Appl., 18: 95-138.

Lesturgie, M., 2011. Some relevant applications of MIMO to radar. Proceedings of the 2011 12th International Symposium on Radar (IRS), September 7-9, 2011, IEEE, Leipzig, Germany, ISBN:978-1-4577-0138-2, pp: 714-721.

Licul, S. and W.A. Davis, 2005. Unified frequency and time-domain antenna modeling and characterization. IEEE. Trans. Antennas Propag., 53: 2882-2888.

Martinez-Vazquez, A. and J. Fortuny-Guasch, 2007. UWB MIMO radar arrays for small area surveillance applications. Proceedings of the 2nd European Conference on Antennas and Propagation (EuCAP 2007), November 11-16, 2007, IET, Edinburgh, UK., ISBN:978-0-86341-842-6, pp: 1-6.

Nion, D. and N.D. Sidiropoulos, 2009. A parafac-based technique for detection and localization of multiple targets in a MIMO radar system. Proceedings of the 2009 IEEE International Conference on Acoustics, Speech and Signal Processing, April 19-24, 2009, IEEE, Taipei, Taiwan, ISBN:978-1-4244-2353-8, pp: 2077-2080.

Schmidt, R.O., 1986. Multiple emitter location and signal parameter estimation. IEEE Trans. Antennas Propagat., 34: 276-280.

Sidiropoulos, N.D. and R. Bro, 2000. On the uniqueness of multilinear decomposition of N-way arrays. J. Chemom., 14: 229-239.

Stegeman, A. and N.D. Sidiropoulos, 2007. On Kruskal's uniqueness condition for the candecomp/parafac decomposition. Linear Algebra Appl., 420: 540-552.